Chapter 5

Sensitivities of the Tropical Pacific Climatology

. . . a sea-change
Into something rich and strange.

Shakespeare, *The Tempest*

5.1 Introduction

In this chapter we examine the sensitivity of the tropical Pacific climatology to perturbations imposed from outside the coupled system. In the real world, such perturbations might arise from changes in the extratropical Pacific, from changes in heating over the continents, or from random fluctuations within the tropics. These would tend to be amplified by coupled feedbacks, similar to those responsible for ENSO and the strong warm pool/cold tongue climatology observed today.

Coupled GCM studies provide another a clear demonstration of this climate sensitivity. Gudgel et al. (2001), for example, found that replacing predicted low-level clouds with observed clouds over tropical landmasses in a global CGCM led to a substantial strengthening of the Walker circulation and east Pacific cold tongue, and a large reduction in the model's climatological bias. This, in turn, had a positive impact on the model's ENSO forecasts. Studies like these point to the need for better simulation of clouds and other poorly-resolved processes, but they also demonstrate the need for better understanding of how errors in these processes are exported to other aspects of the climate system.

Dijkstra and Neelin (1995) explored many aspects of the climate sensitivity of the tropical Pacific using a simplified version of the Zebiak and Cane (1987) coupled model, namely a meridionally-symmetric equatorial strip in the fast-wave limit, neglecting zonal temperature advection and the climatological annual cycle. Arguing that land-sea contrasts and the Coriolis effect on the Hadley cell produce an "external" component of the trade winds, the authors imposed a weak uniform easterly stress in the model which then provided

a seed for coupled feedbacks. The resulting steady-state climatology was found to be very sensitive to the strength of the air-sea coupling. The spatial structure of the climatology was found to depend mostly on internal feedbacks, although the strength of the cold tongue was sensitive to the strength of the externally-imposed trades. The zonal position of the cold tongue depended on a competition between two types of feedbacks: a thermocline feedback, which affected SST east of the stress, and an upwelling feedback, which affected SST in phase with the stress. Since the model stress response lay slightly west of SST extrema, only the thermocline feedback was fully consistent with a cold tongue in the eastern basin; the upwelling feedback tended to drag the cold tongue out into the central basin. The most important role of the externally-imposed easterlies was to generate mean upwelling, which enhanced the thermocline feedback and thereby favored a strong cold tongue in the eastern Pacific.

There remain several unanswered questions. What are the relative roles of equatorial and off-equatorial winds in determining the tropical climatology? Is the mean state more sensitive to wind changes in the east or the west? What is the role of the cross-equatorial southerlies in the eastern Pacific? Are coupled feedbacks sensitive to the nature of the imposed climate perturbation? How do intraseasonal and interannual variability influence the climatology?

This chapter addresses these questions and sets the stage for the study of ENSO sensitivity in Chapter 7. We shall assess both the direct effect of a climate perturbation on the ocean, and the indirect effect that arises from coupled feedbacks with the atmosphere. The direct effect is simulated by forcing the ocean model of Chapter 4 with a prescribed climate change, and allowing the climatology to adjust to this change in the absence of coupling to the statistical atmosphere model. The additional effect of coupling is then simulated by repeating the adjustment experiment with the atmosphere model turned on. In this latter case, the simulation will include ENSO variability (discussed in Chapter 7), so the climatology may include rectified effects of these oscillations.

5.2 Adjustment of the oceanic active layer

5.2.1 Adjustment time scales

The time evolution of the equatorial ocean following a sudden change in wind stress has been studied in detail (Cane and Sarachik 1976, 1977, 1979; Gill 1982; Yamagata and Philander 1985; Philander 1990; Neelin et al. 1998; Philander 1999). Information in the active layer can travel no faster than the equatorial Kelvin mode, which conveys information eastward at the internal gravity wave speed $c = (g'H)^{1/2}$. The next fastest wave is the gravest Rossby mode, which propagates information westward at speed $c/3$. As Fig. 5.1 illustrates, the onset of westerly stress in the active layer model produces Kelvin wave fronts and Rossby wave fronts; the lines crisscrossing the basin correspond to the fronts that emerge from the boundaries immediately after the onset of the winds. The dashed line is the front associated with the initial reflection of Rossby waves at the western boundary; in its wake, the equatorial thermocline shoals and the currents accelerate westward. The solid line is the front associated with the initial reflection of Kelvin waves at the eastern

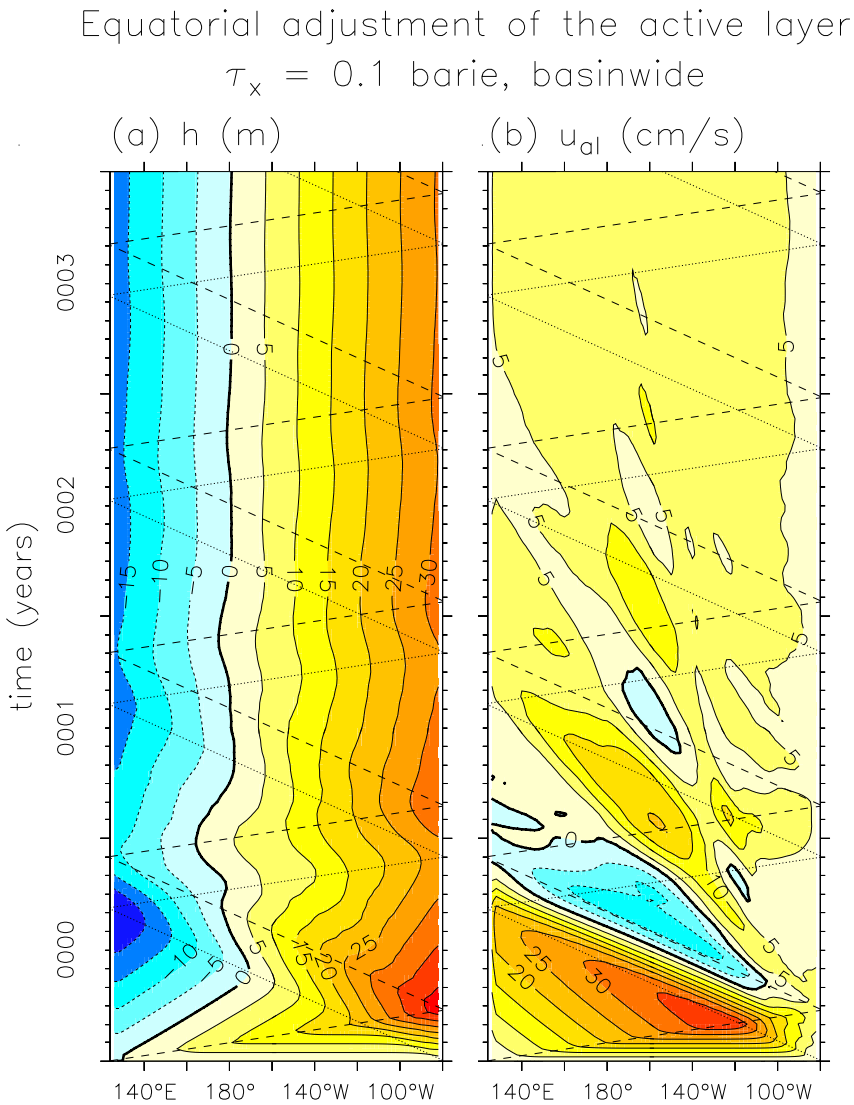

Figure 5.1: Equatorial adjustment of the active layer model to an imposed uniform basin-wide westerly wind stress perturbation of amplitude 0.1 barie. The stress is turned on at $t = 0$ and held constant thereafter. Shown are the simulated perturbation in (a) thermocline depth (m) and (b) active layer zonal current (cm/s). Warm (cool) colors indicate positive (negative) values. Dashed lines correspond to the front associated with the equatorial Kelvin mode emerging from the western boundary at $t = 0$. Dotted lines correspond to the front associated with the gravest Rossby mode emerging from the eastern boundary at $t = 0$. Compare to Fig. 3.18 of Philander (1990).

boundary; in its wake, the equatorial thermocline deepens and the currents accelerate eastward.

The gradual adjustment of the ocean thus proceeds in a series of distinct stages, as the wave fronts cross the basin and reflect at the boundaries. For a basin of zonal width L, the relevant adjustment time scale at the equator is $t_{adjust} = 4L/c$, the time required for one Kelvin-Rossby wave circuit. For the intermediate model, $L = 156°$, $c = 2.42$ m/s and so $t_{adjust} \approx 330$ days. At higher latitudes, the adjustment proceeds more slowly due to the slower speed of Rossby waves, but is nearly complete after two years (Fig. 5.2).

5.2.2 Equilibrium response to uniform westerlies

Fig. 5.3 shows the steady state attained by the active layer after 10 years of continuous forcing by uniform westerly stress. The westerlies have induced a constant zonal slope in the equatorial thermocline, with deepening in the eastern Pacific and shoaling in the western Pacific. This equatorial slope is inhibited by the Newtonian cooling, so that the zonal pressure gradient at the equator does not entirely balance the wind stress. The stress therefore drives steady eastward currents at the equator, which permit viscous friction to complete the zonal momentum budget. The Coriolis force on these currents, which initially had driven a meridional convergence of warm water onto the equator, is now balanced by a poleward pressure gradient force associated with the zonal-mean deepening of the thermocline (and elevation of sea level) at the equator.

Because the boundary reflections are imperfect, zonal currents exist even at the coasts. Mass enters through the western wall via imperfectly-canceled upwelling Rossby waves, and exits through the eastern wall via imperfectly-canceled downwelling Kelvin waves. In the real world, these boundary fluxes would be associated with flow through the Malay Archipelago, and with meridional exchanges via narrow boundary currents.

5.2.3 Response to westerlies with meridional structure

How important are the off-equatorial stresses to the active layer response at the equator? To answer this question, the ocean model is spun up as in the previous section, except that the zonal stress perturbation now has the form

$$\overline{\tau}_x^* = \widetilde{\overline{\tau}_x^*} e^{-y^2/L_y^2} \tag{5.1}$$

i.e., it is constant in the zonal direction, and has a Gaussian shape in the meridional with an equatorial maximum of $\widetilde{\overline{\tau}_x^*}$.

Fig. 5.4 shows how the equilibrium active layer climatology depends on the meridional halfwidth L_y of the zonal stress, when the equatorial stress is held constant. The intriguing result is that the response of the equatorial climatology is sensitive to the off-equatorial structure of the stress. The zonal-mean equatorial thermocline shoals for narrow westerlies, but deepens for wide westerlies. Away from the equator, the zonal-mean thermocline response is the opposite, indicating a net transfer of heat content from the equator to the off-equator (for narrow westerlies) or vice versa (for wide westerlies). Narrow westerlies also produce a stronger eastward zonal-mean current response at the equator, in addition to off-equatorial zonal-mean countercurrents which are absent for wide westerlies.

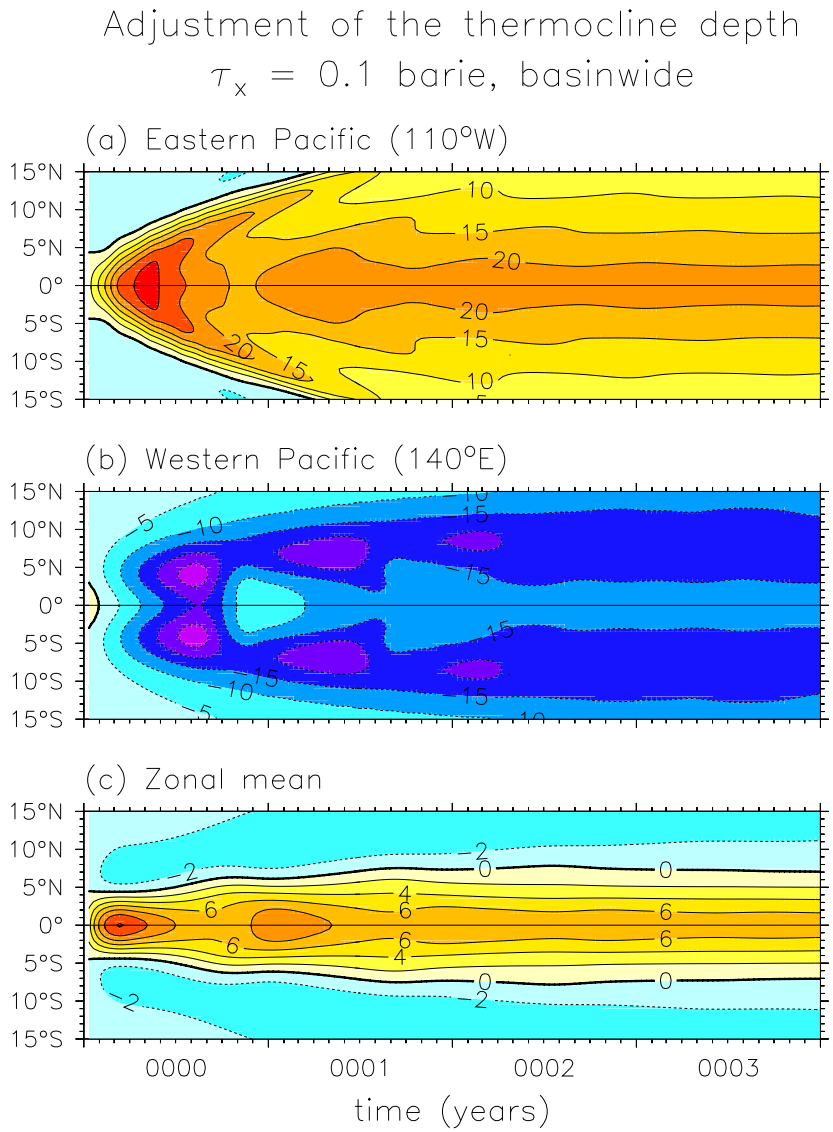

Figure 5.2: Adjustment of the thermocline depth to a uniform basin-wide westerly stress of amplitude 0.1 barie that is turned on at time $t = 0$. Latitude/time diagrams of the thermocline depth perturbation (m) are shown for (a) the eastern Pacific at 110°W, (b) the western Pacific at 140°E, and (c) the basin zonal average.

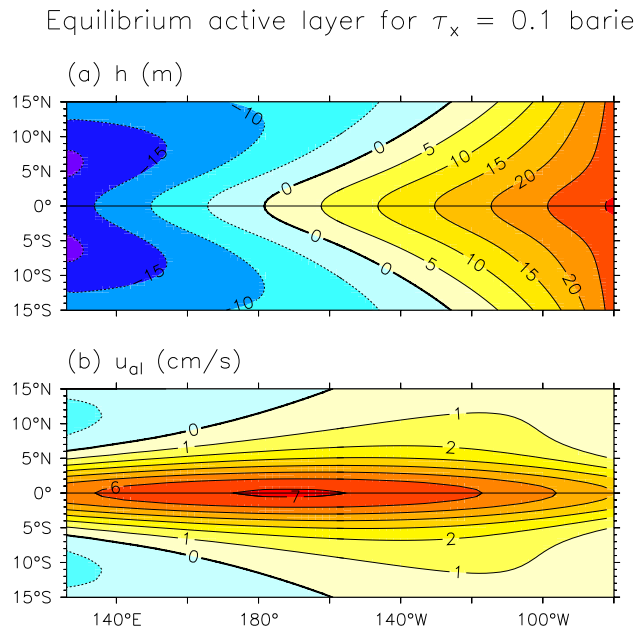

Figure 5.3: Equilibrium active-layer perturbation achieved following 10 yr of forcing by uniform basin-wide westerly stress of amplitude 0.1 barie. (a) Thermocline depth (m), (b) zonal current (cm/s).

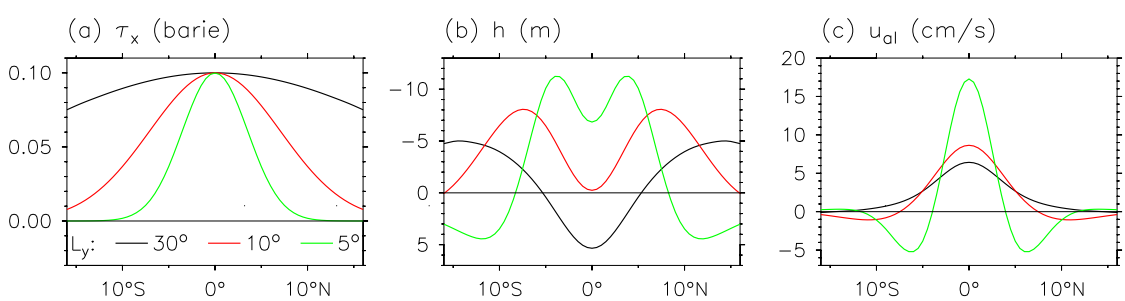

Figure 5.4: Simulated zonal-mean equilibrium response of the active layer to an imposed westerly stress perturbation of amplitude 0.1 barie, which is zonally constant and has a meridionally Gaussian shape with an e-folding halfwidth of 30° (black), 10° (red), and 5° (green). (a) Imposed zonal stress, (b) equilibrium thermocline depth, (c) equilibrium zonal current.

These results can be understood by considering the steady-state vorticity budget of the active layer. The zonal-mean depth of the equatorial thermocline is determined by a competition between equatorial Ekman pumping and off-equatorial Ekman suction. The former, generated directly by the equatorial westerlies, induces vortex squashing, equatorial convergence, and therefore acts to deepen the equatorial thermocline. The latter, generated by cyclonic curl on the poleward flanks of the stress, induces vortex stretching and poleward flow off-equator, which produces a divergence of water from the equatorial zone and therefore acts to shoal the equatorial thermocline. For a narrow perturbation (small L_y), the off-equatorial Ekman suction dominates and the equatorial thermocline shoals. For a wide perturbation (large L_y), the equatorial Ekman pumping dominates and the equatorial thermocline deepens. Note that there is also some effective zonal mass flux through the boundaries, identified with boundary currents and gaps in the coastline; for westerly stress, the western boundary acts as a source of mass at the equator while the eastern boundary is a sink. At intermediate L_y these three effects cancel and the zonal-mean equatorial thermocline depth is unchanged. For the boundary reflectivities assumed by the model, the critical width of zonal stress for which the zonal-mean thermocline feels no net effect is $L_y \approx 10°$ latitude.

The local deepening of the thermocline near the equator, which is due to equatorial Ekman pumping, is associated with nearly geostrophic zonal currents that are eastward on the poleward flanks of the warm bulge. The off-equatorial cyclonic stress curl, on the other hand, induces a local shoaling of the thermocline, which is associated with currents that are eastward on the equatorward flank of the cold dip and westward on the poleward flank. As L_y decreases, the edges of the westerly stress perturbation draw closer to the equator and sharpen, so that the cyclonic curl near the equator intensifies. Thus meridionally-narrow westerlies give rise to strong equatorial eastward currents, and to westward zonal-mean countercurrents a few degrees away from the equator.

That the equator responds differently to narrow and wide stress perturbations is important, because both types of forcing are present in the real world. The wide-stress case is analogous to the climatological easterlies (Fig. 2.1), which actually *strengthen* away from the equator; this positive off-equatorial curl assists the equatorial Ekman divergence in shoaling the equatorial thermocline. The narrow-stress case resembles the El Niño anomalous stress (Fig. 3.7), which has $L_y \approx 8°$. The equilibrium thermocline response to such narrow stress consists of a zonal-mean shoaling at the equator, and since this shoaling opposes the thermocline deepening in the eastern Pacific observed during El Niño, it has been argued that the equatorial ocean's slow approach to equilibrium (associated with the discharge of equatorial heat content) may be responsible for ENSO (Jin 1997).

Note that since this recharge/discharge is achieved through the formation and western boundary reflection of oceanic Rossby waves, it is fully compatible with earlier "delayed oscillator" ideas (Battisti 1988; Suarez and Schopf 1988) in which wave reflections from the western boundary play a key role. The role of western boundary reflections is simply to cancel enough of the Rossby flux to allow interior geostrophic divergence to control the zonal-mean equatorial thermocline depth.

It is important to understand how changes in equatorial versus the off-equatorial stress

might affect ENSO, since both components are susceptible to model differences and long-term climate variability. The equatorial component of the stress is tightly linked to the warm pool/cold tongue climatology of the ocean, which is very sensitive to changes in external forcings or changes in model dynamics (Dijkstra and Neelin 1995). The off-equatorial component is more directly tied to strength of the Hadley circulation, which not only differs among climate models (Delecluse et al. 1998; AchutaRao et al. 2002) but also may be subject to future climate change (Rind 1987; Dai et al. 2001). Section 5.4 will thus explore the relative effects of equatorial and off-equatorial stress changes on the tropical Pacific climatology.

5.3 Design of the climate sensitivity experiments

As indicated by Fig. 5.2, the tropical ocean is very nearly in equilibrium with wind stress variations that occur on time scales longer than a few years. Thus if a given climate parameter is slowly changed during a model run, the simulated climatology will approximately be in equilibrium with that change. This approach is convenient, since only a single run of the model is required, and it is also highly relevant to many kinds of GCM experiments, in which slow variations in anthropogenic or orbital forcings cause changes in climate.

Thus the climate sensitivity experiments are performed as follows. The background state of the anomaly model is in all cases prescribed from the control run climatology described in Section 4.2.4. A climate perturbation is selected, along with a range of parameter values to be tested. An ocean-only climate simulation is then performed by first spinning up the ocean anomaly model for 10 years with the parameter start value, and then running the ocean model for another 500 years as the parameter changes linearly from the start value to the end value. This procedure is then repeated with the statistical stress anomaly model and noise turned on in a fully coupled climate simulation. A control case is also performed by running the coupled stochastic model for 500 years with no climate perturbation imposed. "Noiseless" coupled experiments were also performed, but as these were found to produce climatologies very similar to (though slightly more sensitive than) those in the stochastic cases, they will not be discussed except in connection with Fig. 5.5.

5.4 Changes in mean zonal stress

5.4.1 Equatorial stress

How does the equatorial climatology response to a change in the equatorial trade winds? In nature and in coupled models, such a change could arise due to a change (or model error) in the strength of the Hadley circulation or land-sea temperature contrast, or from a change (or model error) in the effective air-sea coupling of the tropical climate system (Dijkstra and Neelin 1995).

In our first experiment, a perturbation of the form (5.1) with $L_y = 15°$ is imposed in the intermediate model, and the stress amplitude $\widetilde{\overline{\tau}_x^*}$ is linearly varied from -0.1 to 0.1 barie over the course of a 500 year simulation. Fig. 5.5 shows the resulting change in

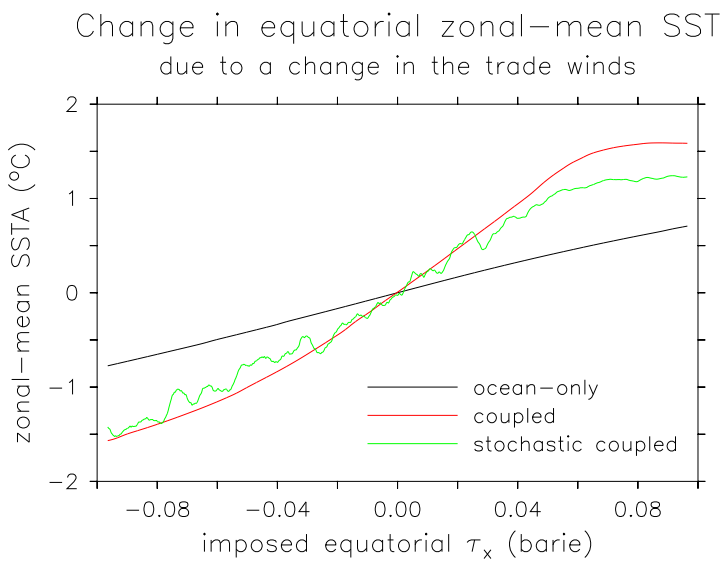

Figure 5.5: Simulated change in the zonal-mean equatorial (2°S–2°N) SST climatology resulting from an imposed equatorial zonal stress perturbation, which is zonally constant and has a meridionally Gaussian shape with an e-folding halfwidth of 15°. Horizontal axis is the strength of the imposed stress perturbation; vertical axis is the SST response. Shown are the response of the uncoupled ocean (black), the coupled ocean/atmosphere without noise (red), and the coupled system with noise (green). All curves are filtered to eliminate periods shorter than 20 years.

zonal-mean equatorial SST for the ocean-only, coupled, and stochastic coupled cases. In all cases the equatorial band warms as the trade winds weaken. The warming is greatest in the coupled cases, where nonlinear saturation is evident for very weak or very strong trades. The coupled system appears to be less sensitive with noise than without.

The equatorial structure of the ocean-only and stochastic coupled cases are shown in Fig. 5.6. The plotted curves represent equatorial 50-year averages from the beginning and end of the sensitivity runs, so that the time averages are centered on ±0.09 barie. To facilitate comparison with later figures, all data have been scaled by the peak equatorial SST change in the stochastic coupled case, indicated above panel (b). The model surface heat flux may be obtained from (b) by multiplying by a factor of $-\epsilon$. Mixing also tends to oppose SST anomalies in the model, though its effect is smaller than the surface heat flux. Note also that the equilibrium equatorial zonal current in the model looks very similar to τ_x, while the equatorial upwelling looks very similar to $-\tau_x$.

Uncoupled oceanic response

Focusing first on the westerly ocean-only case in Fig. 5.6 (plain red lines), we see that as in Fig. 5.3, zonally-constant equatorial westerlies induce a constant zonal slope in the equatorial thermocline. The deepening of the thermocline in the east is associated with warmer water below the mixed layer, especially in the far eastern Pacific where the mean

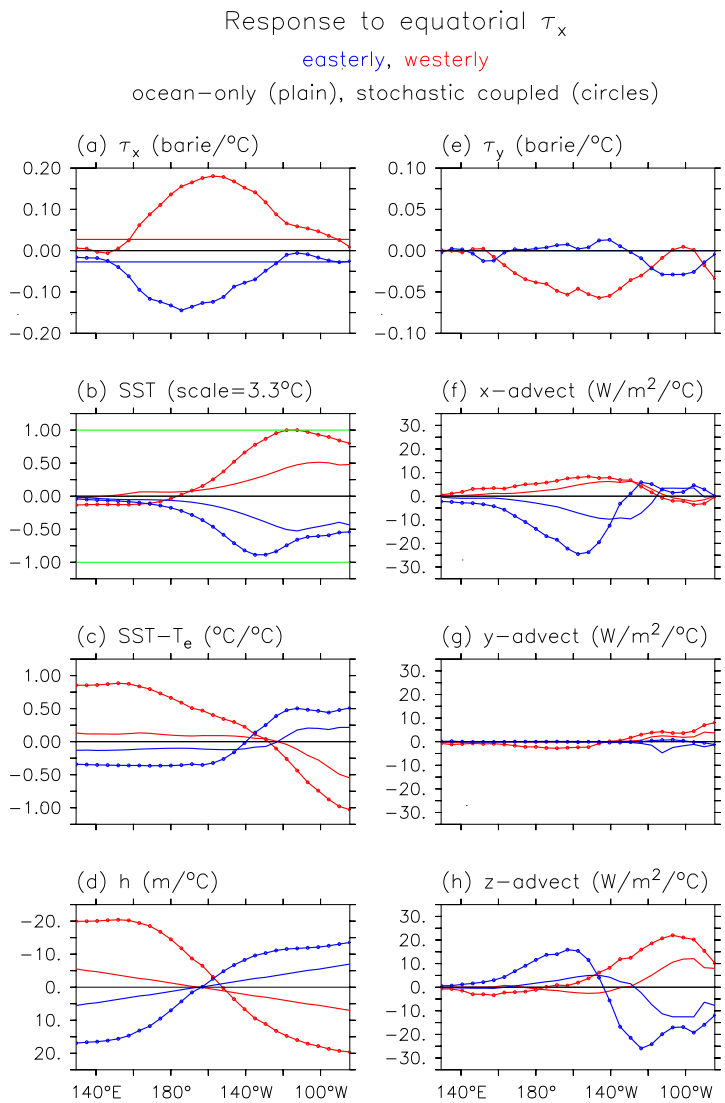

Figure 5.6: Simulated response of the equatorial (2°S–2°N) climatology to an imposed equatorial zonal stress perturbation of amplitude 0.09 barie, which is zonally constant and has a meridionally Gaussian shape with an e-folding halfwidth of 15°. Red (blue) lines correspond to a westerly (easterly) stress perturbation. Plain lines indicate the ocean response without coupled feedbacks, circled lines the response of the coupled ocean/atmosphere with noise. Fields are scaled by the peak SST change in the coupled case, indicated in panel (b). Panels show the scaled change in (a) zonal stress, (b) SST, (c) temperature difference across the mixed layer, (d) thermocline depth (ordinate reversed), (e) meridional stress; and the mixed layer heating due to (f) zonal, (g) meridional, and (h) vertical advection.

thermocline is shallow. The increase in subsurface temperatures in the east gives a reduced vertical temperature gradient, which produces an eastern warming of SST as warmer water is entrained into the mixed layer from below.

The weakening of the trades also weakens the westward advection of cold water, warming the surface the central Pacific where the mean zonal SST gradient is strong. The surface warming by zonal advection outpaces the increase in T_e, and the vertical temperature gradient steepens. Despite the reduction of upwelling in the central Pacific, the strong increase in $\partial_z T$ results in a net increase in cooling by vertical advection, which mitigates some of the zonal advective warming in the central Pacific.

The effect of meridional advection at the equator is weak, although it does induce some warming in the east as northward currents advect the southern warming (associated with upwelling induced by the cross-equatorial southerly stress, Appendix C) into the equatorial band. Off-equator, meridional advection plays a larger role: there it warms SST as reduced poleward Ekman flow gives anomalously weak meridional spreading of the cold tongue.

An easterly stress perturbation gives largely the opposite response (plain blue lines). In particular, because the active layer model is linear, the thermocline response is exactly opposite from that in the westerly case. Compared to the westerly case, however, the entrainment temperature change in the easterly case is only half as strong in the east, since the T_e parameterization (Fig. 4.7) saturates when the thermocline shoals beyond the model mixed layer depth; cooling is then limited by the temperature of water below the thermocline. Slightly farther west, T_e responds more strongly than in the westerly case, as the thermocline approaches the mixed layer depth from below. Thus T_e west of 110°W reacts more strongly to *strengthening* trades, while T_e east of 110°W reacts more strongly to *weakening* trades. In the central Pacific, zonal advection responds more strongly in the easterly case, as intensified currents carry even colder water westward.

It is interesting to note that despite the strong nonlinearity of the vertical temperature gradient response (c) at the eastern boundary, the vertical advection response at the eastern boundary is nearly linear. For weakened trades the vertical advection response is limited by a lack of equatorial upwelling, while for strengthened trades it is limited by the saturation of T_e. Since the south-equatorial upwelling associated with the cross-equatorial southerlies is unaffected by the imposed zonal stress perturbation, the saturation of T_e is more evident in the southeast than at the equator. This nonlinearity is carried across the equator by the northward currents in the east, limiting the meridional advection response at the equator in the easterly case. Off-equator in the central Pacific (not shown), the sensitivity to the easterly perturbation is enhanced due to a combination of stronger meridional overturning and a stronger poleward temperature gradient.

In summary, the uncoupled SST response to weakening trades is narrower and more asymmetric meridionally, and lies further to the east, than the response to strengthening trades. *Weakening* trades strongly reduce *vertical* temperature gradients in the far eastern Pacific, inducing large changes in vertical advection just south of the equator. *Strengthening* trades strongly enhance *horizontal* temperature gradients in the tropical Pacific, inducing large changes in horizontal advection at the equator. For weak winds, horizontal advection in the central basin is limited by elimination of the cold tongue. For strong winds, vertical advection in the east is limited by saturation of the entrainment temperature when the

thermocline becomes too shallow in the east.

Coupled response

What effect does coupling have on this response? It is obvious from Fig. 5.6 that coupled feedbacks play a major role. Panel (b) indicates that the peak SST change in the equatorial band is nearly twice as strong when coupled (circled lines) than when uncoupled. Considering the rather small change in zonal stress (typical of, say, the difference between observational stress analyses in Fig. 2.1a), the induced SST change is quite large.

Over the central basin, the coupled zonal wind stress response is much larger than the imposed perturbation, and the stronger change in zonal stress produces a larger thermocline slope than in the uncoupled case. Because the coupled stress response is narrow in the meridional (Fig. 3.7), the zonal mean thermocline perturbation is opposite to that in the uncoupled cases, and slightly opposes the thermocline perturbation in the eastern Pacific. The larger thermocline slope in the coupled cases gives rise to a stronger, and more nonlinear, change in the vertical temperature gradient in the eastern Pacific; the T_e nonlinearity produces a vertical advection response which is shifted west in the easterly case relative to the westerly case.

In the central basin, zonal advection is little affected by the coupling in the westerly case; the eastward current anomalies have little effect since the zonal gradient of SST is nearly zero. In the easterly case, however, zonal advection is strongly amplified by the coupling since stronger currents are acting on an increased SST gradient; this produces an intense cooling in the central Pacific which tends to drag the cold tongue westward. This so strongly reduces the vertical temperature gradient that vertical advection acts to damp the cooling in the central basin, despite the stronger vertical currents in the easterly case. Vertical advection thus acts to temper some of the nonlinearity associated with zonal advection in the central Pacific.

The meridional stress response at the equator, shown in panel (e), is weak but highly nonlinear. The SST response in the case with imposed easterlies is nearly symmetric about the equator, so that the cross-equatorial southerlies are little changed. The case with imposed westerlies, on the other hand, shows more warming south of the equator than north of the equator, and the warming response is confined to the eastern Pacific. This pattern of warming corresponds to a strong negative projection onto mode 2 of the wind stress model (Fig. 3.8), and therefore acts to weaken the equatorial southerlies in the central Pacific. It is possible that additional coupled feedbacks not explicitly included in the simulation (e.g. stratus clouds, evaporative heat fluxes) might enhance the asymmetry of the climate response in the real world. This asymmetry, in turn, could be expected to alter the evolution of the annual cycle, which is closely tied to the strength of the climatological southerlies (Chang and Philander 1994; Li and Philander 1996; Li and Hogan 1999; Wang and Wang 1999).

The net effect of these coupled feedbacks and nonlinearities is to give an SST response in the easterly case which is farther west than in the westerly case. Using the terminology of recent ENSO literature (Hao et al. 1993; Jin and Neelin 1993a; Neelin et al. 1998; Fedorov and Philander 2000; An and Wang 2000; An and Jin 2001), the effects of coupling on the mean state may be described in terms of "nonlocal" or thermocline feedbacks ($-\overline{w}\partial_z T'$)

and "local" or zonal advective/upwelling feedbacks ($-u'\partial_x T$ and $-w'\partial_z T$). The former are consistent with an SST response in the east while the latter tend to drag the response westward (Dijkstra and Neelin 1995). The nonlinearity of T_e favors the thermocline feedback when the thermocline is at intermediate depths, shallow enough to affect entrainment but not so shallow that T_e saturates at the temperature of sub-thermocline waters. The nonlinearity of the zonal advective product $-u'\partial_x T'$, on the other hand, increasingly favors local feedbacks as the cold tongue strengthens and $\overline{T}_x$ increases. The response to easterlies favors local feedbacks over thermocline feedbacks, allowing the SST response to slide west relative to the westerly case.

Fig. 5.6, therefore, establishes three fundamental ideas: (1) coupling strongly amplifies the climate response to perturbations; (2) this enhances nonlinearities which alter the climatological SST budget; (3) these nonlinearities affect the spatial structure of the coupled climate response.

5.4.2 Off-equatorial stress

In the next experiment, we explore the sensitivity of the climatology to a change in the off-equatorial zonal wind stress, which in Section 5.2.3 was shown to be important in the adjustment of active layer. In nature and in coupled models, such a change could arise due to a change in the strength of the Hadley circulation or land-sea temperature contrast. In the intermediate model, a perturbation of the form

$$\overline{\tau}_x^* = \widetilde{\overline{\tau}_x^*}\left(1 - e^{-y^2/L_y^2}\right) \tag{5.2}$$

is imposed with $L_y = 15°$. This perturbation is constant in the zonal direction, zero at the equator, and has an inverted Gaussian shape in the meridional with an off-equatorial maximum of $\widetilde{\overline{\tau}_x^*}$. In other words, it is what one would add to the perturbation (5.1) of the previous section to give a uniform τ_x over the basin.

Because the perturbation has no signature at the equator, it cannot directly affect the strength of equatorial upwelling or the equatorial zonal slope of the thermocline. It can, however, directly affect equatorial climate by changing the zonal-mean depth of the thermocline and the zonal current at the equator, which feel the influence of off-equatorial stress through interior divergence and the boundary conditions (4.5)–(4.6). This experiment thus provides a useful analogue for other processes that could affect the zonal-mean depth of the equatorial thermocline in the real world, such as changes in the thermohaline circulation or changes in subduction in high midlatitudes (Gu and Philander 1997).

Following the previous experiment, the stress amplitude $\widetilde{\overline{\tau}_x^*}$ is linearly varied from -0.1 to 0.1 barie over the course of a 500 year simulation. Results for the ocean-only and stochastic coupled cases are shown in Fig. 5.7. The plotted curves represent equatorial 50-year averages from the beginning and end of the sensitivity runs, so that the time averages are centered on ± 0.09 barie. As in Fig. 5.6, all data have been scaled by the peak equatorial SST change in the stochastic coupled case, indicated above panel (b).

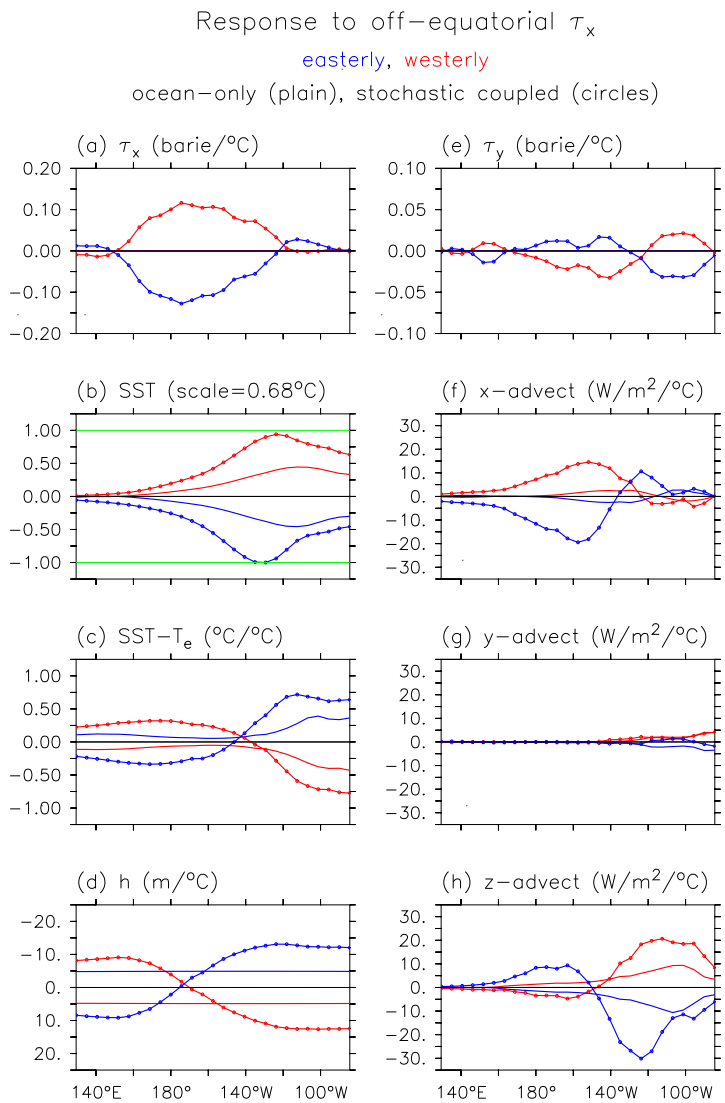

Figure 5.7: Simulated response of the equatorial climatology to an imposed off-equatorial zonal stress perturbation. The perturbation is zonally constant, vanishes at the equator, and has an inverted Gaussian shape in the meridional with an e-folding halfwidth of 15° and a peak off-equatorial amplitude of 0.09 barie. Red (blue) lines correspond to a westerly (easterly) stress perturbation. Otherwise as in Fig. 5.6.

Uncoupled oceanic response

How much does the off-equatorial wind stress affect the equatorial SST? Focusing first on the westerly ocean-only case in Fig. 5.7 (plain red lines), we see that off-equatorial westerlies induce a zonal-mean deepening of the equatorial thermocline, without changing its zonal slope. The deepening warms the surface by allowing warmer water to be entrained into the mixed layer, especially in the eastern Pacific where the climatological thermocline is shallow. These processes are very similar to the case with equatorial westerlies, although the amplitude of the changes is weaker in this case due to the smaller change in the eastern equatorial thermocline depth.

There is slightly reduced cooling from zonal advection in the central basin, due to a weakening of the easterly currents as the thermocline flattens in the meridional. The increase in T_e as a result of the thermocline deepening in the central basin, however, is strong enough to overcome the zonal advective surface warming, and so produces a reduction in $\partial_z T$ and a vertical advective warming tendency in the central Pacific (in contrast to Fig. 5.6). The change in meridional advection at the equator is even weaker than in Fig. 5.6, since there is little change in the Ekman currents due to absence of any wind stress change at the equator.

Off-equatorial easterlies gives nearly the opposite response (plain blue lines), with an equatorial shoaling of the thermocline and a cooling in the eastern Pacific. There is some nonlinearity evident in the vertical temperature gradient in the east, but it less prominent than in the equatorial-stress case since the overall response is weaker.

Thus the key results from the off-equatorial uncoupled cases are that (1) off-equatorial stress perturbations are felt at the equator, and (2) the zonal asymmetry of the background climatology, namely the shoaling of the thermocline to the east, produces a zonally-asymmetric change in SST even given a zonally-uniform change in equatorial thermocline depth.

Coupled response

How well does the off-equatorial wind stress seed coupled feedbacks? It is again evident that coupled feedbacks greatly amplify the climate response, by a factor of two or more (circled lines). Off-equatorial westerlies produce an eastern warming, which generates a "feedback" westerly stress anomaly at the equator. Because these feedback westerlies are meridionally narrow, they generate equatorial divergence and so the zonal-mean thermocline does not deepen as much as in the uncoupled case. More important, however, is the stronger deepening in the east (where entrainment is most sensitive to thermocline depth) associated with the thermocline slope in the coupled case. Although the feedback stress has a smaller amplitude than the off-equatorial stress, it is very efficient at generating additional climate changes due to its direct equatorial influence on upwelling, zonal currents, and the zonal slope of the thermocline.

It is striking how similar the coupled responses in Fig. 5.7 are to those in Fig. 5.6 (although nonlinearity is not as evident in the present case because the coupled response is weaker). Both cases show a coupled response with roughly the same structure and advective balance, and an SST response to easterlies that is shifted slightly west of the

response to westerlies. Since the coupled feedbacks are so large, the ultimate structure of the coupled response appears largely invariant to the seed perturbation. In this sense, the coupled feedbacks greatly simplify the problem of describing the climate response to external forcing. That the tropical Pacific has a preferred ENSO-like response pattern suggests that one could define a "tropical Pacific climate index" to characterize the climatology as either "El Niño-like" or "La Niña-like". Indeed, in Figs. 5.6 and 5.7 we have already used such an index (the maximum SST change along the equator) to scale the climatological fields for comparison. The problem is then reduced to understanding the sensitivity of this single index.

Thus the key result from the off-equatorial coupled cases is that latitude of the zonal stress perturbation is not essential to structure of the response; more important are the equatorial coupled feedbacks. Neelin and Dijkstra (1995) and Dijkstra and Neelin (1995) provide a firm foundation for understanding of how these coupled feedbacks affect the zonal structure of the climatology. The *amplitude* of the coupled response, on the other hand, *does* depend critically on the seed perturbation, as can be seen by comparing the SST scales in Figs. 5.6 and 5.7; off-equatorial stress is less efficient than equatorial stress at producing equatorial climate changes. In the next section, we quantify this statement by comparing equatorial and off-equatorial zonal stress forcings of different meridional widths.

5.4.3 Meridional width of the stress

Equatorial stress

How sensitive is the climatology to the detailed meridional structure of the climatological zonal stress? To answer this question, the intermediate model is subjected to an equatorial zonal wind stress of the form (5.1), and the meridional width L_y of the perturbation is linearly varied from 5° to 30° over the course of a 500 year simulation. The amplitude $\widetilde{\overline{\tau}_x^*} = 0.1$ barie is held constant in time and is the same for all cases. Model results for the ocean-only and stochastic coupled cases are shown in Fig. 5.8.

Panel (a) indicates that coupled feedbacks substantially amplify the eastern equatorial SST response, and these feedbacks are nonlinear, i.e. the feedback warming for westerlies is greater than the feedback cooling for easterlies. The SST is rather insensitive to the meridional width of the perturbation, indicating that it is the equatorial value of the stress perturbation that dominates the climate response. The SST is slightly less sensitive to narrow imposed stress, because narrow stress induces a zonal-mean thermocline depth change (panel b, see also Fig. 5.4) which in the east opposes the depth change due to the thermocline slope.

The coupled feedback zonal stresses are meridionally narrow (Figs. 3.7–3.8), and so induce an additional shoaling of the zonal-mean thermocline for westerlies, and additional deepening for easterlies. These zonal-mean thermocline changes help to limit the coupled SST response by opposing the slope-related thermocline changes in the east. Compared to the zonally-asymmetric changes, however, the zonal-mean changes are clearly of secondary importance in determining the overall effect on SST. In the westerly case, for example, coupling enhances the surface warming despite a shoaling of the zonal mean thermocline.

The feedbacks also amplify the zonal currents along the equator (panel c of Fig. 5.8).

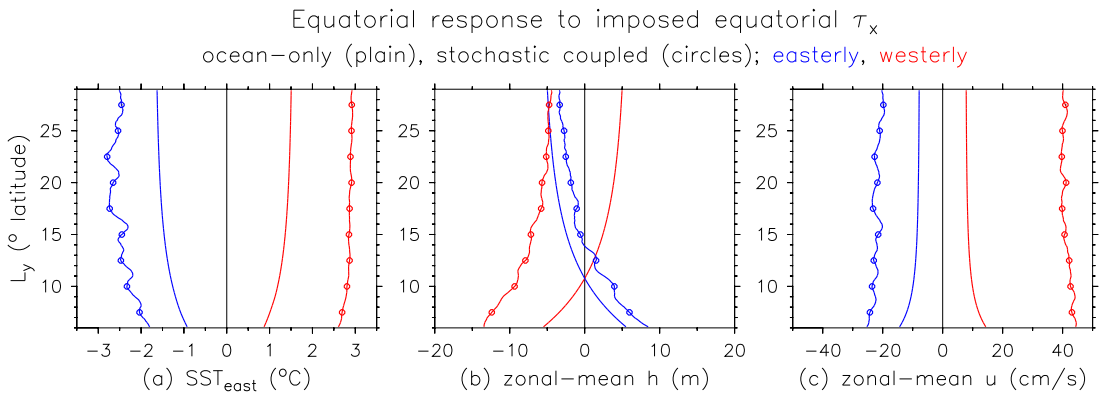

Figure 5.8: Simulated response of the equatorial (2°S–2°N) climatology to an imposed equatorial zonal stress perturbation of amplitude 0.1 barie, which is zonally constant and has a meridionally Gaussian shape with an e-folding halfwidth of L_y. Red (blue) lines correspond to westerly (easterly) stress perturbations. Plain lines indicate the ocean response without coupled feedbacks, circled lines the response of the coupled ocean/atmosphere with noise. Panels show the long-term mean changes, relative to the control case, of (a) SST averaged over the eastern Pacific (150°W–90°W), (b) zonal-mean thermocline depth, and (c) zonal-mean mixed layer zonal current.

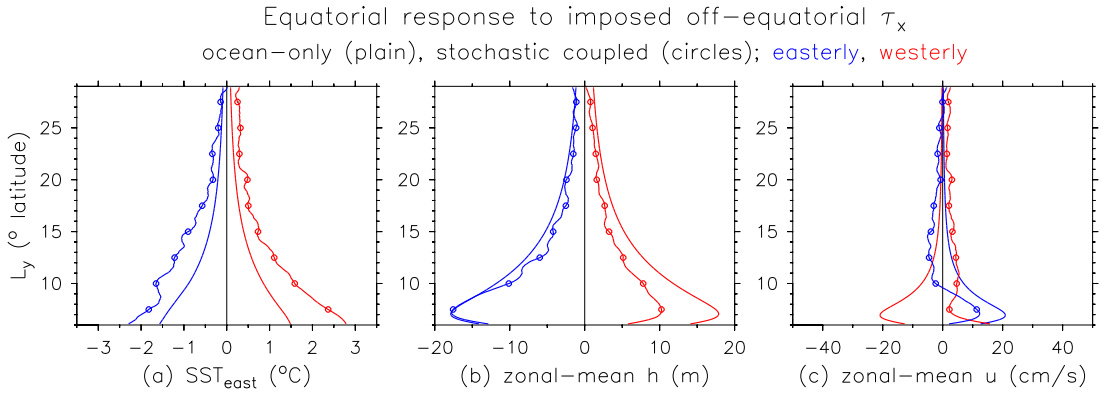

Figure 5.9: Simulated response of the equatorial (2°S–2°N) climatology to an imposed off-equatorial zonal stress perturbation which is zonally constant, vanishes at the equator, and has an inverted Gaussian shape in the meridional with an e-folding halfwidth of L_y and a peak off-equatorial amplitude of 0.1 barie. Otherwise as in Fig. 5.8.

The effect of coupling on the equatorial zonal-mean thermocline and zonal currents is greatest in the westerly case, because the pattern of SST warming, which is more zonally and meridionally asymmetric than the pattern of cooling, projects more strongly onto mode 2 of the statistical atmosphere (Fig. 3.8) which gives strong cyclonic stress curl in the equatorial eastern Pacific. The feedback westerlies are in effect meridionally "narrower" than the feedback easterlies. Thus the coupled westerly case shows a greater change in the equatorial zonal-mean thermocline and zonal current than does the coupled easterly case. The thermocline change is the more important for SST; e.g. in the westerly case SST warms with increasing L_y despite the slightly weakening current perturbation.

In summary, the SST response is not very sensitive to the meridional width L_y of an imposed equatorial τ_x perturbation. The zonal-mean thermocline depth, on the other hand, *is* sensitive to L_y and also to the width of the feedback stress. The zonal-mean zonal currents are likewise sensitive to L_y. It is therefore possible for two climatologies with similar SSTs to have very different zonal-mean structures below the surface. Such climatologies may also have different mixed layer heat budgets, since widening the stress enhances the effect of thermocline changes on SST, while narrowing the stress enhances the effect of zonal current changes on SST.

Off-equatorial stress

Repeating the experiment instead with a purely off-equatorial zonal wind stress of the form (5.2) results in Fig. 5.9. Here the only way the stress perturbation can affect the equatorial region is by altering the zonal-mean currents and thermocline depth. Panel (c) indicates that the current changes are rather small for all L_y, so the most important effect of off-equatorial westerlies is to induce a deepening of the zonal-mean thermocline at the equator, which then causes a warming of the eastern Pacific that is amplified by coupled feedbacks.

The SST change is strongest when the edges of the imposed stress are close to the equator, so that the near-equatorial stress curl is intense; the SST change in the uncoupled cases is roughly twice as strong for $L_y = 10°$ than for $L_y = 15°$. Narrow stress creates strong Sverdrup divergence, which then strongly affects the zonal-mean thermocline and plants a large seed for equatorial coupled feedbacks to grow. Since the feedback stress is meridionally narrow, it "fills in" the equatorial gap in the imposed stress, canceling part of the zonal-mean response. This is especially the case for the feedback westerlies, since they are narrower than the feedback easterlies.

Comparing Fig. 5.9 to Fig. 5.8, we see that the uncoupled SST responses to off-equatorial and equatorial perturbations are comparable for $L_y \approx 8°$. Coupling, however, is more effective at amplifying the response in the equatorial-stress case, since that case has additional equatorial upwelling and slope-related eastern thermocline depth perturbations generated directly by the imposed stress.

In summary, the tropical Pacific climatology is most sensitive to the part of a zonal stress perturbation that lies on the equator; it is not very sensitive to the part of the stress that is far from the equator. Purely off-equatorial stress perturbations can, if they are near enough to the equator, induce large equatorial changes by affecting the zonal-mean thermocline depth, but off-equatorial stress is less effective than equatorial stress at seeding

coupled feedbacks because it does not induce changes in equatorial upwelling or the zonal slope of the thermocline.

5.4.4 Longitude of the stress

Given the zonal asymmetry of the tropical Pacific climatology and the coupled feedback response, does a change in wind stress forcing in the eastern Pacific affect the climatology differently than a change in the western Pacific? To address this question, we investigate the sensitivity of the climatology to the longitude of an equatorial zonal stress perturbation. In the intermediate model, a bivariate Gaussian perturbation of the form

$$\overline{\tau}_x^* = \widetilde{\overline{\tau}_x^*} \exp\left[-\frac{(x-x_0)^2}{L_x^2} - \frac{y^2}{L_y^2}\right] \tag{5.3}$$

is imposed with $L_x = 40°$ and $L_y = 15°$. This perturbation has an equatorial maximum of $\widetilde{\overline{\tau}_x^*}$ at longitude x_0.

We start by characterizing the structure of the forced and coupled responses to westerly stress perturbations in the east and west. The stress amplitude is held constant at 0.1 barie, and x_0 is linearly shifted from 125°E to 85°W over the course of a 500 year simulation. Results for the ocean-only and stochastic coupled cases are shown in Fig. 5.10. The plotted curves represent equatorial 50-year averages centered on $x_0 = 170°$E and $x_0 = 130°$W. As in Fig. 5.6, all data have been scaled by the peak equatorial SST change in the stochastic coupled case, indicated above panel (b).

Uncoupled oceanic response

The plain lines in Fig. 5.10 show the uncoupled responses of the equatorial ocean climatology to westerly stress perturbations in the eastern Pacific (case E hereafter) and western Pacific (case W hereafter). The thermocline slope is in zonal phase with the stress, so in case W the thermocline deepens over a large region of the eastern basin, while in case E it deepens only in the east.

These different thermocline responses, together with the stronger change in upwelling in the eastern Pacific in case E, induce changes in $\partial_z T$ and vertical advection that are zonally shifted relative to each other in the same sense as the stress, i.e. case W gives vertical advective warming that lies slightly west of that in case E. Since case E therefore produces a stronger change in $\partial_x T$, it exhibits a stronger central Pacific warming from zonal advection than does case W, but the effect of this zonal advective change is mitigated in case E by increased vertical advective cooling in the central Pacific. The net result is that case E has a stronger warming in the east but a weaker warming in the west.

Coupled response

Coupled feedbacks substantially alter this picture. Compared to the uncoupled responses, the coupled responses (circled lines in Fig. 5.10) look much more similar to each other, since the position of the feedback stress is determined mostly by the model dynamics and is much stronger than the imposed perturbation. As in the uncoupled regime, the SST

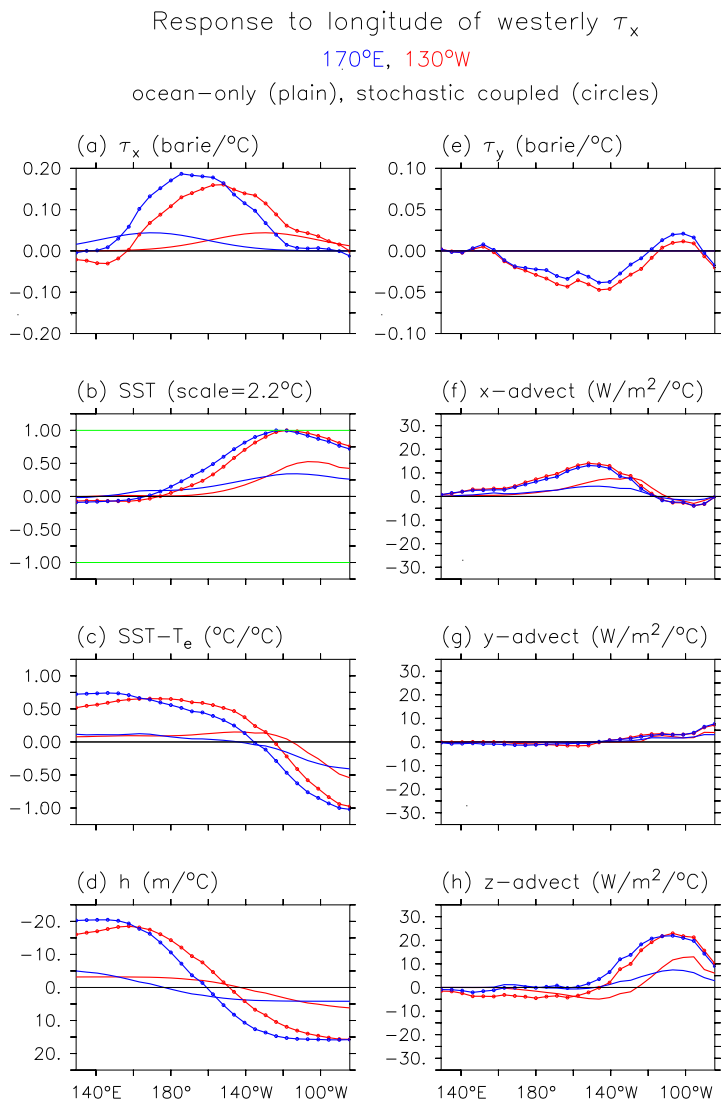

Figure 5.10: Simulated response of the equatorial climatology to an imposed equatorial westerly stress perturbation that is zonally localized. The perturbation has a peak equatorial amplitude of 0.1 barie and a bivariate Gaussian shape with e-folding halfwidths of 40° longitude and 15° latitude. Red (blue) lines correspond to a westerly perturbation with a peak at 130°W (170°E). Otherwise as in Fig. 5.6.

response in case E is shifted eastward of that in case W, but relative to the total SST change the shift is very slight, and the peak SST changes are nearly identical in the two cases. There is also little difference between the advective terms in cases E and W, and the meridional stress change, which is due entirely to coupled feedbacks, is nearly identical between the two cases. It is again evident that the spatial structure of the coupled feedbacks is little affected by the structure of the imposed perturbation, as long as that perturbation is not excessively large. The primary role of the forcing, regardless of zonal position, is to seed coupled feedbacks which then determine the spatial structure of the climatology.

Despite the similarities in the SST climatologies, however, there are important dynamical differences between cases E and W which will be relevant to ENSO variability. This is because the external perturbations persist in the adjusted wind stress, i.e. they are not canceled by the coupled feedbacks. Compared to case E, case W has stronger anomalous westerlies in the west and so shows a stronger deepening of the thermocline over the entire central and eastern Pacific, along with a stronger reduction in $\partial_z T$. Case W also maintains stronger upwelling in the east, as indicated by lack of any westerly anomalies there. Since these fields control the strength of the thermocline feedback and local feedbacks, one can anticipate that the climatologies for E and W (which look rather similar on the surface) may produce quite different ENSO behavior.

Experiments with imposed *easterly* stress perturbations were also performed (not shown). Compared to the westerly experiments, the coupled response in case W is shifted farther to the west of case E. This is because the zonal advective and T_e saturation nonlinearities grow more important as the climatology becomes more La Niña-like (Fig. 5.6). The thermocline is nearer to the surface in the east, and so SST becomes more sensitive to the differences in the thermocline structure associated with the different stress positions. The zonal SST gradient is also stronger in the easterly cases, so the SST also becomes more sensitive to the position of the zonal currents which underlie the stress perturbations.

Longitude of peak zonal stress sensitivity

Where along the equator is the climatology most sensitive to a zonal stress perturbation? Fig. 5.11 shows how the ocean-only and coupled responses depend on the zonal position x_0 of a westerly perturbation. We consider first the ocean-only case (top row). The first column shows the imposed westerly forcing; the equatorial downwelling and zonal current perturbations (not shown) are in zonal phase with and slightly west of the stress, respectively. As the westerlies shift eastward, the zonal slope of the equatorial thermocline shifts eastward, and the zonal extent of deep h in the east decreases. The zonal fetch of the stress perturbation, and therefore the east-west thermocline depth difference, is greatest when x_0 is in the center of the basin. The peak thermocline response in the east occurs for $x_0 \approx 160°$W.

It is interesting to note that when the westerlies in the west, they deepen the zonal-mean h, but when they are in the east, they shoal the zonal-mean h. To understand why, let us consider the wave signals arriving at a point in the center of the basin. For wide stress (here $L_y = 15°$) the equatorial Kelvin signals generated in the region of forcing are stronger than the off-equatorial Rossby signals, so the equatorial response is dominated by the former. When x_0 is in the west, h receives a fresh Kelvin deepening signal arriving

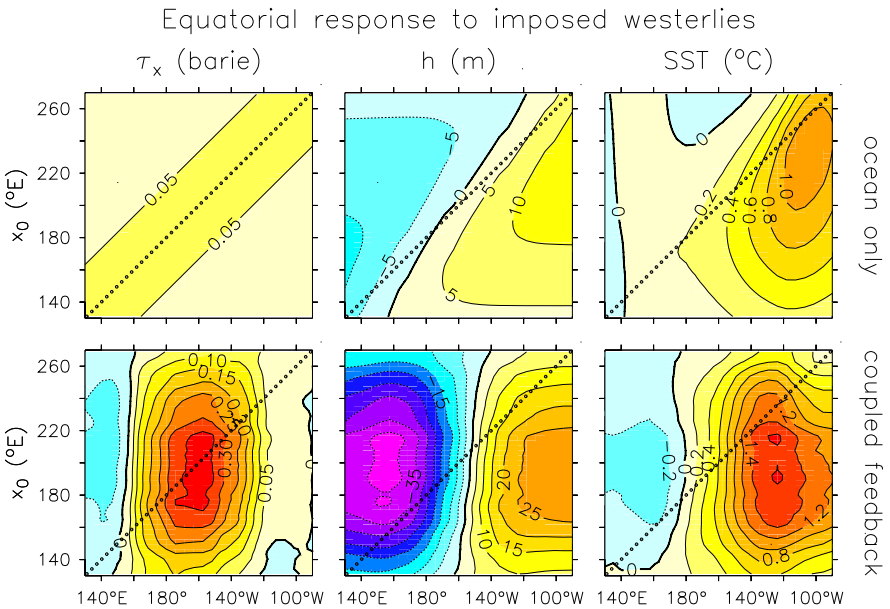

Figure 5.11: Change in the equatorial (2°S–2°N) climatology resulting from a Gaussian westerly stress perturbation with halfwidths of 40° longitude and 15° latitude and a peak value of 0.1 barie on the equator at longitude x_0 (circles). Left column gives the zonal stress change, center column the thermocline depth change, right column the SST change. Top row shows the forcing and response in the ocean-only case, bottom row the added feedback in the stochastic coupled case. Warm (cool) colors indicate positive (negative) values.

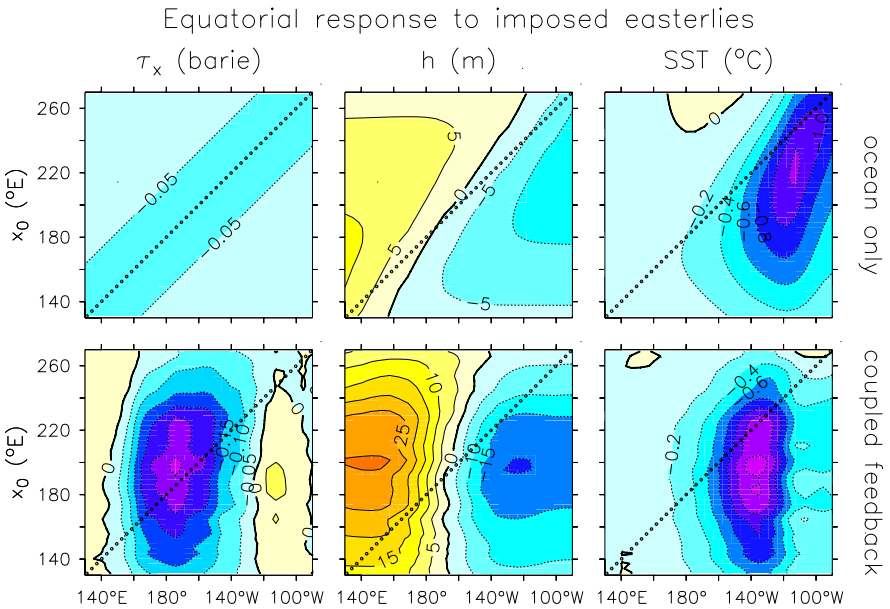

Figure 5.12: As in Fig. 5.11, but for an easterly imposed perturbation.

directly from the region of westerly forcing. When x_0 is in the east, h receives this signal only after a leaky eastern boundary reflection a long Rossby-wave transit westward during which the signal is damped, and a leaky western boundary reflection. These arguments hold at all points interior to x_0, so the zonal-mean thermocline ends up deeper in the case with x_0 in the west than in the east.

As x_0 shifts eastward, the SST response strengthens and becomes more trapped in the east. The peak responses of the SST and its zonal gradient occur for $x_0 \approx 130°$W. When x_0 is very far east, cooling develops in the central basin, where the thermocline shoals but there is little downwelling to oppose the cooling since the westerlies are so far east.

How does coupling affect this picture? The bottom row of Fig. 5.11 shows the air-sea feedback effect in the stochastic coupled case. The feedback response is stronger than the forced response, and consists of peak westerlies near 160°W, and peak warming near 130°W. Strikingly, the position of the feedback response is nearly independent of the position of the westerly forcing: as x_0 crosses the basin from west to east, the feedback stress and thermocline depth shift eastward by less than 20° longitude, and the feedback SST hardly shifts at all. The spatial structure of the feedbacks again appears to be set by the internal dynamics of the coupled system, not the position of the forcing.

The *amplitude* of the feedbacks, however, does depend strongly on x_0. The feedbacks are strongest when the stress forcing lies near the center of the basin ($x_0 \approx 155°$W). Since this is close to the longitude of the feedback stress, it implies that the best seed perturbation for coupled feedbacks is simply one that looks like the feedbacks themselves. Recall that the SST response in the uncoupled case was most sensitive to stress forcing in the eastern Pacific ($x_0 \approx 130°$W). The key point is that *the coupled ocean is sensitive to wind stress forcing in a different location than the uncoupled ocean.*

Fig. 5.12 repeats the experiment but for imposed easterlies instead of westerlies. It is again evident that the coupled feedbacks are very important, that their spatial structure is relatively insensitive to the longitude of the forcing, and that their amplitude is maximized when the forcing lies in the center of the basin. Compared to the case with westerly forcing, however, the forced response in this easterly case is slightly stronger and the coupled feedbacks are slightly weaker. The responses also lie slightly farther west in this case, since zonal advection, which operates mainly in the central basin, plays a larger role when the cold tongue is strong. Unlike the case with westerly forcing, the western Pacific SST has the same sign as that in the east, due to the stronger influence of zonal advection. The SST response is limited in the east by feedback westerlies, which induce local downwelling that reduces the surface cooling.

5.5 Changes in radiative forcing

How does the tropical Pacific climate respond to changes in surface heating that arise from errors in simulated heat fluxes, or from anthropogenic changes in the real world? Given the observed increase in global-mean surface temperature over the past century, and given the accumulation of greenhouse gases in the atmosphere which may drive future climate change, it is worthwhile to examine the possible impacts of such radiative changes on the tropical Pacific.

In the next experiment we impose a uniform heat flux over the entire basin, with an amplitude ranging between -20 Watt m^{-2} (cooling) and 20 Watt m^{-2} (warming) over the course of a 500 year simulation. Results for the ocean-only and stochastic coupled cases are shown in Fig. 5.13. The plotted curves represent equatorial 50-year averages centered on fluxes of ± 10 Watt m^{-2}. As in Fig. 5.6, all data have been scaled by the peak equatorial SST change in the stochastic coupled case, indicated above panel (b).

Uncoupled oceanic response

The plain red line in Fig. 5.13 shows the uncoupled response of the equatorial ocean climatology to imposed heating. The warming is greatest off-equator (not shown) and in the western Pacific, where the ocean circulation is weak and the imposed heating can only be balanced by an increase in the heat flux out of the ocean. This is accomplished through the linear damping term in (4.18), which represents the effect of increased evaporation from the sea surface. In the eastern equatorial Pacific, however, the heating is also balanced by vertical advection (panel h), which has a greater cooling effect due to the increased vertical temperature gradient associated with the warmer SST. Upwelling serves as a "dynamical thermostat" in the east (Clement et al. 1996), so that the eastern equatorial Pacific warms less than the western equatorial Pacific. The eastern equatorial cooling is exported to the western Pacific by zonal advection (panel f) and to the off-equator by meridional advection (not shown). For imposed cooling (plain blue line), the uncoupled response of the ocean is precisely opposite.

Coupled response

Are the homogenizing effects of coupled feedbacks evident for perturbations other than zonal stress? The fascinating thing about Fig. 5.13 is that the coupled feedbacks utterly dominate the response at the equator. In the imposed-warming case (circled red line), the strengthening of the zonal SST contrast by uncoupled processes gives rise to stronger easterlies, which produce greater upwelling at the equator and an even stronger SST contrast. The net result is that the entire equatorial central and eastern Pacific actually *cool down* in the presence of imposed uniform heating. The patterns of the coupled heat flux response are nearly identical in form, mechanism, and nonlinearity to the zonal stress responses shown in Fig. 5.6. An imposed uniform heating of 10 Watt m^{-2} has roughly the same effect on equatorial SST in the model as imposed zonally-uniform equatorial easterly stress of magnitude 0.06 barie.

This cooling of the equatorial Pacific in response to imposed uniform heating has been noted in other intermediate coupled models (Dijkstra and Neelin 1995; Clement et al. 1996) and in observations (Kaplan et al. 1998). However, it is not reproduced by the current generation of GCMs, perhaps because weak equatorial upwelling, diffuse simulated thermoclines, and weak air-sea coupling reduce the effects of dynamical feedbacks in those models (Cane et al. 1997). The key point from Fig. 5.13 is that coupled feedbacks may be very important to the climate response at the equator, so it is important to get these feedbacks right if we are to trust model projections of tropical climate changes and the ENSO response to those changes.

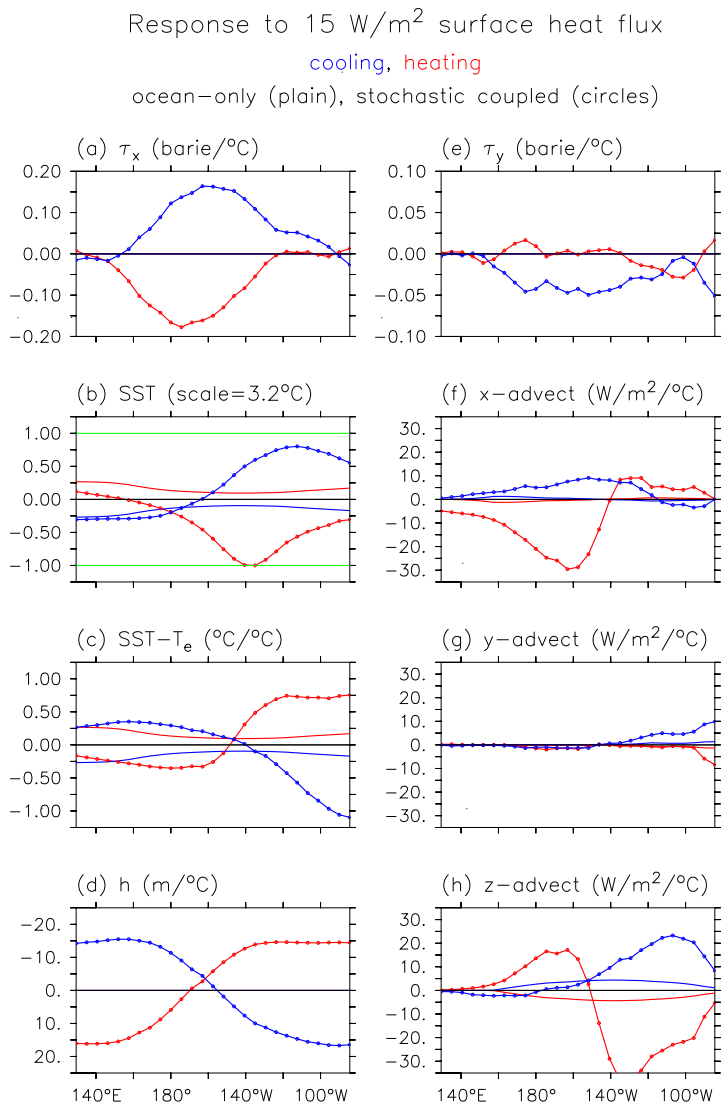

Figure 5.13: Simulated response of the equatorial climatology to an imposed uniform heat flux of 10 Watt m^{-2}. Red (blue) lines correspond to imposed basin-wide heating (cooling). Otherwise as in Fig. 5.6.

5.6 Changes in mean meridional wind stress

The meridional asymmetry of the eastern tropical Pacific mean state results from an ocean-atmosphere instability closely tied to the annual cycle (Philander et al. 1996; Wang and Wang 1999). The meridional wind stresses ($\overline{\tau}_y$) associated with this climate instability are important, because they generate upwelling south of the equator in the eastern Pacific (Appendix C). This enhances SST/thermocline coupling in that region, in a manner similar to what happens when the zonal trade winds shift eastward (Section 5.4). Thus it is reasonable to expect that a change in the cross-equatorial southerlies might affect ENSO. In nature and in coupled models, such a change might arise due to a change in the land-sea temperature contrast, cloud feedbacks, or the seasonal cycle.

In this section we examine the effect of such a change on the tropical Pacific climatology. In the intermediate model, a meridional stress perturbation is imposed with the form

$$\overline{\tau}_y^* = \widetilde{\overline{\tau}_y^*} \exp\left[-\frac{(x-x_0)^2}{L_x^2} - \frac{y^2}{L_y^2}\right] \tag{5.4}$$

This perturbation is a bivariate Gaussian, with an equatorial maximum of $\widetilde{\overline{\tau}_y^*}$ at longitude x_0. Values of $L_x = 40°$, $L_y = 20°$, and $x_0 = 100°$W correspond roughly to the position and shape of the annual-mean climatology of cross-equatorial southerlies in the eastern Pacific. The stress amplitude $\widetilde{\overline{\tau}_y^*}$ is varied from -0.1 to 0.1 barie over the course of a 500 year simulation. Results for the ocean-only and stochastic coupled cases are shown in Fig. 5.14. The plotted curves represent equatorial 50-year averages from the beginning and end of the sensitivity runs, so that the time averages are centered on ± 0.09 barie. As in Fig. 5.6, all data have been scaled by the peak equatorial SST change in the stochastic coupled case, indicated above panel (b).

Uncoupled oceanic response

The uncoupled response of the active layer to the strengthened southerlies (plain red line) resembles that for the uniform change in meridional stress studied by Cane and Sarachik (1977) and Yamagata and Philander (1985); it consists entirely of antisymmetric Rossby waves, which in this case are confined near the eastern boundary especially at high latitudes. The thermocline shoals slightly in the southeast Pacific, and the westward currents intensify in the cold tongue region south of the equator. There are also important changes in the Ekman layer: upwelling increases south of the equator, and there is enhanced cross-equatorial transport in the eastern Pacific.

Together, these changes effect a strengthening of the cold tongue, as more and colder water is upwelled south of the equator, and more of this water is carried northward across the equator. Zonal advection also acts to cool the eastern Pacific by advecting the anomalously cold waters westward. Because the southerly stress perturbation has no effect on *equatorial* upwelling or the equatorial thermocline depth, the changes in vertical advection at the equator are due entirely to the change in SST induced by horizontal advection. Vertical advection thus acts as a damping on the equatorial SST anomalies. For southerly stress the SST cooling is mostly confined to the far eastern Pacific. The SST response to

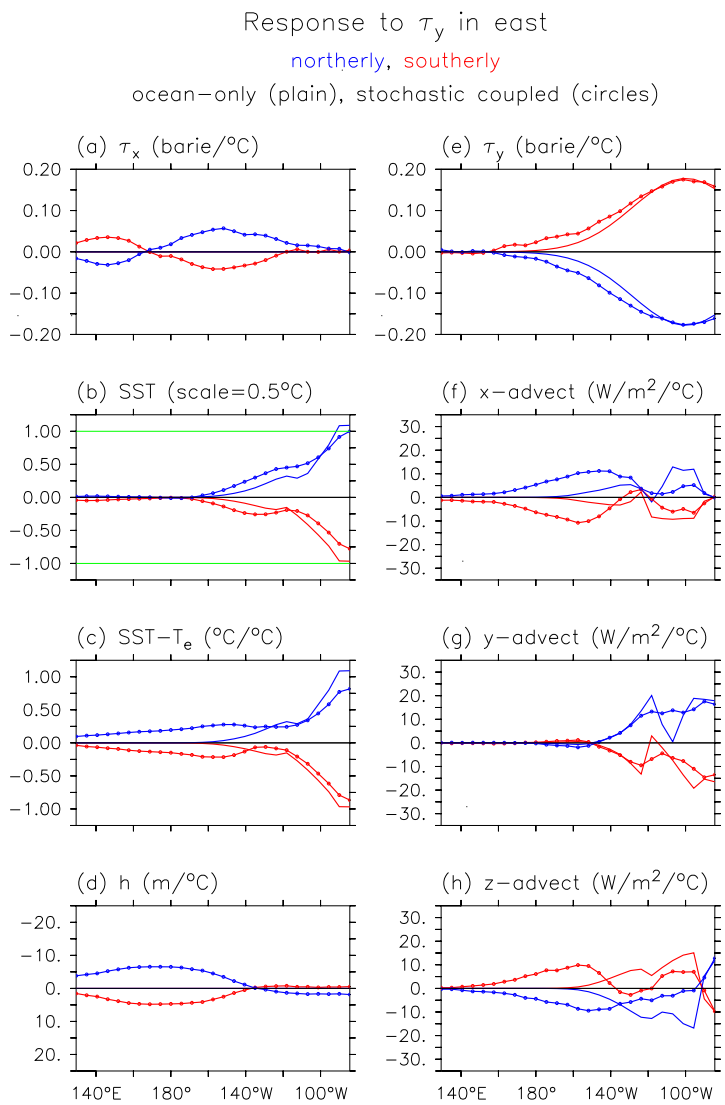

Figure 5.14: Simulated response of the equatorial climatology to an imposed meridional stress perturbation in the eastern equatorial Pacific. The perturbation has a peak amplitude of 0.09 barie on the equator at 100°W, and a bivariate Gaussian shape with e-folding halfwidths of 40° longitude and 20° latitude. Red (blue) lines correspond to a southerly (northerly) stress perturbation. Otherwise as in Fig. 5.6 except that the ordinate of panel (e) has been changed.

northerly stress is almost exactly opposite, with a warming in the far eastern Pacific; the small amplitude of the response makes the dynamics nearly linear.

Coupled response

We have shown that a wide variety of climate perturbations can produce similar coupled feedbacks, which homogenize the net response. Are these feedbacks universal? Not entirely—the striking thing about Fig. 5.14 is that meridional stress induces very little coupled feedback in the model. The forced SST pattern induced by the meridional stress projects only weakly on the SST patterns of the statistical atmosphere, which are linked more to the observed ENSO zonal stress. Thus there is little feedback generated in either the meridional or the zonal stress. For the zonal stress feedback that *does* arise, there is very little stress in the east (so there is little change in equatorial upwelling in the east), and the fetch in the western Pacific is canceled by that in the central Pacific (so the thermocline depth is nearly unchanged in the east). As a result, vertical advection plays little role except to damp the perturbations induced by horizontal advection.

In the central Pacific, the zonal stress feedback induces slight upwelling changes that enhance the changes induced by the forcing; e.g. in the case of stronger southerlies the τ_x feedback is easterly at the equator and so induces upwelling, which cools the SST in addition to the cooling tendency from stronger southerly-induced upwelling south of the equator. In the western Pacific, the warming by vertical advection (acting on a deepened thermocline) almost exactly cancels the cooling by zonal advection, so that there is almost no change in SST.

Thus the effect of southerly stress on the equatorial climatology of the model is fairly small, is confined to the southeastern Pacific, and produces almost no coupled feedbacks. This is in stark contrast to Figs. 5.6, 5.7, and 5.10, in which the coupled feedbacks dominated the response. Thus, not all climate perturbations are alike: the "seed" perturbation planted by meridional stress does not grow nearly as well as that planted by zonal stress. It should be noted, however, that additional feedbacks not explicitly included in the simulation, such as stratus cloud shading, vertical mixing in the ocean, and evaporative heat fluxes, might enhance the asymmetry of the coupled climate response in the real world.

Despite the small sensitivity of the model to changes in τ_y, it is important to note that the response to meridional stress has a rather different spatial structure than the full climatology. Southerlies shift the upwelling south of the equator and strengthen it, while northerlies do the opposite. This change in the strength and asymmetry of the upwelling, and the additional changes in the structure of the thermocline depth, could be expected to alter the spatial patterns and stability of ENSO variability.

5.7 Sensitivity of a hybrid coupled GCM

In this section, we turn to a more sophisticated model to study the tropical Pacific response to climate changes. The model is a statistical-dynamical hybrid, consisting of a state-of-the-art ocean GCM coupled to a statistical model of the atmosphere. A description of the model and an analysis of a control run are presented in Appendix F. The purpose of

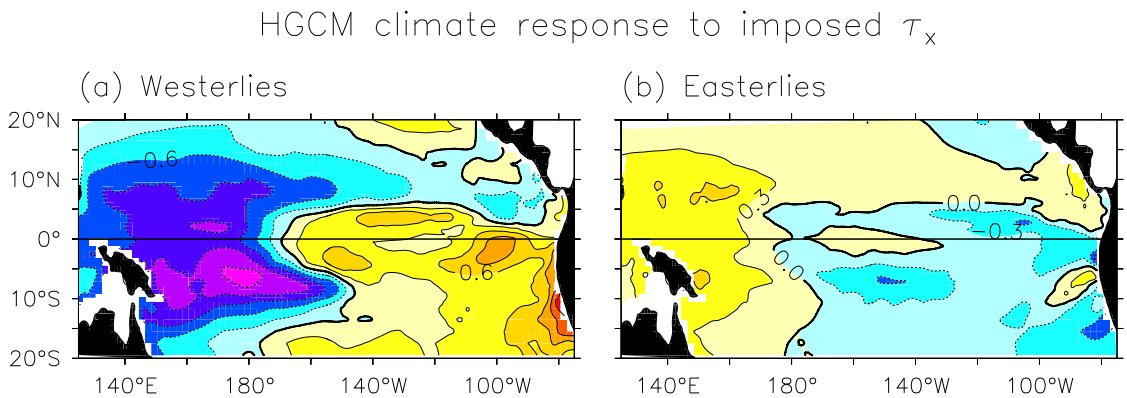

Figure 5.15: Response of the annual-mean tropical Pacific SST climatology to an imposed zonal stress perturbation, as simulated by a hybrid coupled GCM. The imposed perturbation has a peak amplitude of 0.1 barie on the equator at 140°W and a bivariate Gaussian shape with e-folding halfwidths of 40° longitude and 15° latitude. (a) Imposed westerlies, (b) imposed easterlies. Contour interval is 0.3°C; warm shading indicates a warming, cool shading a cooling.

this section is to show that the GCM has its own unique sensitivity to climate perturbations, though some of the insights gained from the intermediate model apply to this system as well.

5.7.1 Changes in mean zonal stress

We first perform a pair of GCM runs to test the sensitivity of the climatology to a change in equatorial zonal stress. Recall that in the intermediate model, this perturbation was analogous to a whole host of other possible perturbations. Following the model initialization, a zonal stress perturbation of the form (5.3) is imposed with $L_x = 40°$, $L_y = 15°$, $x_0 = 140°$W, and $\widetilde{\overline{\tau}_x^*} = \pm 1$ barie. The GCM takes some time to adjust to this change, so the first four years of each run are discarded and the climatology is computed only for the subsequent 16 years. Subtracting the control-run climatology then gives the simulated climate response to the easterly and westerly perturbations.

The change in annual-mean SST for each case is shown in Fig. 5.15. In the westerly case, there is a general weakening of the cold tongue/warm pool contrast, with a warming in the eastern equatorial and southeastern tropical Pacific, and a cooling in the west. The warming is strongest off the coast of Peru, and extends westward along the equator to about 170°W; note that most of the warming occurs off-equator, not on the equator. The cooling in the west is meridionally broad and peaks about 5° south of the equator near the dateline. In the easterly case, the zonal SST contrast strengthens, though the SST change is much weaker than in the westerly case.

The equatorial structures of the responses are shown in Fig. 5.16. As in Fig. 5.6, all data have been scaled by the peak equatorial SST change, indicated above panel (b). As in the intermediate model, it is apparent that coupled feedbacks are important in amplifying

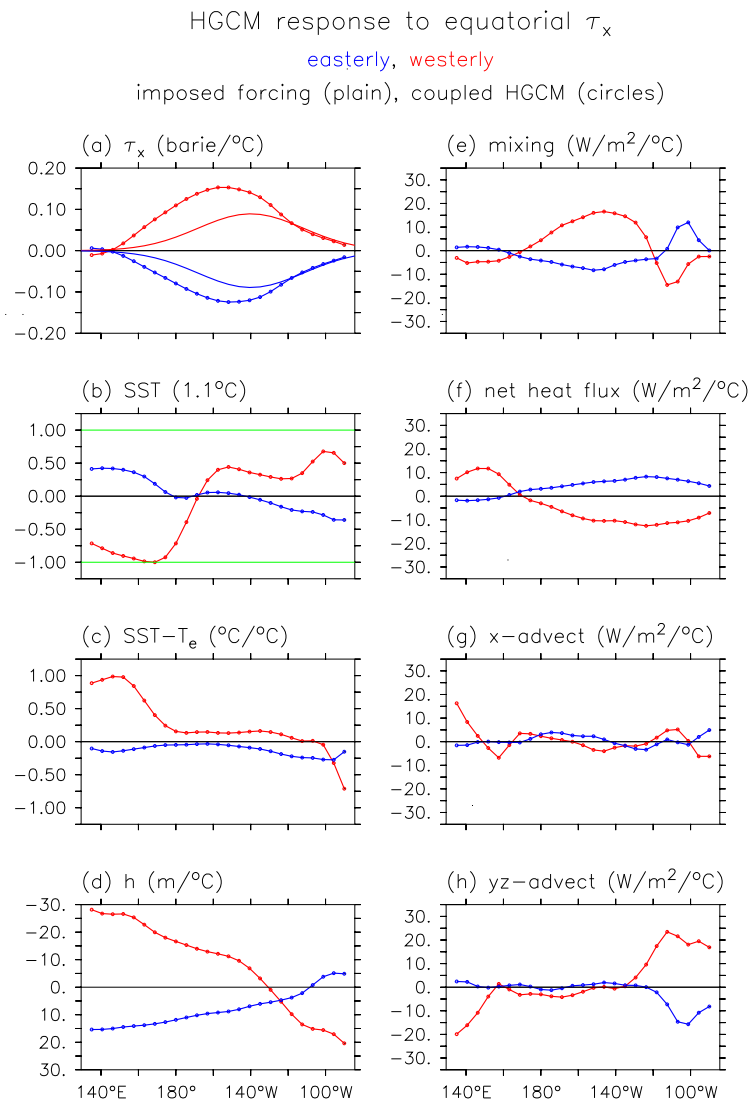

Figure 5.16: Response of the equatorial (2°S–2°N) climatology to an imposed equatorial zonal stress perturbation, as simulated by a hybrid coupled GCM. The imposed perturbation (plain lines in panel a) has a peak amplitude of 0.1 barie on the equator at 140°W and a bivariate Gaussian shape with e-folding halfwidths of 40° longitude and 15° latitude. Red (blue) lines correspond to a westerly (easterly) stress perturbations. Fields are scaled by the peak SST change indicated in panel (b). Panels show the scaled change in (a) zonal stress, (b) SST, (c) temperature difference across the top 50 m, (d) depth of the 20°C isotherm (ordinate reversed); and the mixed layer heating due to (e) eddy fluxes, (f) surface fluxes, (g) zonal advection, and (h) meridional plus vertical advection.

and modifying the response; the coupled zonal wind stress is about 15° farther west than the imposed forcing. However, the climatological SST response and coupled feedbacks at the equator are only about half as strong as in the intermediate model.

For imposed westerlies, there is some thermocline deepening in the eastern Pacific, but its weakening effect on $\partial_z T$ is overcome by the surface warming except very near the eastern boundary. The weakening of the trades, however, reduces upwelling at and south of the equator, which warms the surface through vertical and meridional advection. This change is opposed in the east by a weakening of the eddy fluxes, which means that less warm off-equatorial is stirred into the equatorial band. In the central Pacific, on the other hand, the change in the eddy flux contributes to the surface warming. (In the control case, the eddy flux had a net cooling effect in the central basin, while in this case it has a net warming effect.) The warming in the central and eastern basin are opposed by an increase in the surface heat flux. In the western and central Pacific, the thermocline shoals strongly, which causes a large increase in $\partial_z T$ in the west and a slight increase in the central basin. In those regions the Ekman currents act on the stronger gradients to cool the surface. Note that there is little change in zonal advection, except for a moderate warming effect in the far western basin which opposes the cooling effects of entrainment and eddy fluxes. The net result of these complex changes is a rather unusual-looking change in SST, with a fairly weak warming plateau in the east, dropping off rapidly to a stronger cooling in the west. The climatological zonal SST gradient is thus weakened for the case with imposed westerlies.

Imposed easterlies have a much smaller effect on the thermocline, but it is interesting to note that h ends up deeper almost everywhere except in the far eastern basin. There is also very little change in the vertical temperature gradient apart from a general weakening all along the equator. In the far eastern basin, stronger upwelling acts to cools the surface despite the weakening of $\partial_z T$. This cooling is balanced by increased eddy warming in the east and decreased heat flux out of the ocean. In the central Pacific, the SST decreases mostly due to a heightened eddy cooling, which is balanced by reduced heat flux out of the ocean. In contrast to the case with imposed westerlies, this case shows little change in the heat balance in the western Pacific. However, the SST warms significantly in the west, since in this region the surface flux does not supply much damping. As in the westerly case, the effect of zonal advection is fairly small. The net result of these changes is a slight increase in the zonal SST contrast.

Thus there are some general similarities with the intermediate model results: in the imposed-westerly case the thermocline flattens, the zonal SST gradient weakens, and the westerlies are enhanced by the coupling; in the imposed-easterly case the opposite happens but the coupled feedbacks are weaker. However, the GCM also shows many differences with the intermediate model. First, the responses are weaker and the $\partial_z T$ changes are smaller in the east, especially in the easterly case. Note that the weaker responses may be partly due to the use of only a single mode in the GCM statistical atmosphere; the SST change patterns are quite different between the easterly and westerly cases, with the latter projecting more strongly onto the leading regression mode. Second, the temperature changes in the west are stronger than in the east. Third, changes in the eddy fluxes play a larger role, while zonal advection and surface fluxes play smaller roles. The HGCM

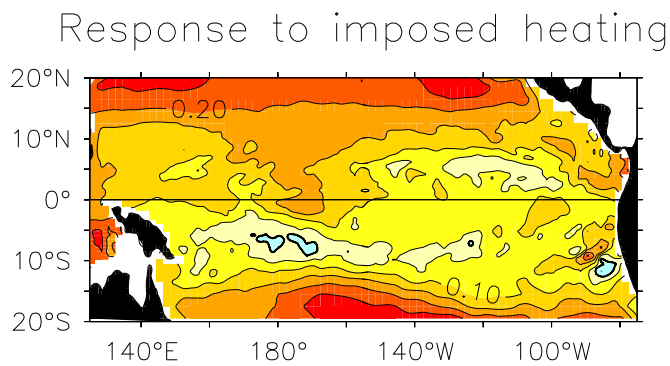

Figure 5.17: Response of the annual-mean tropical Pacific SST climatology to an imposed uniform 1 Watt m^{-2} heating perturbation, as simulated by a hybrid coupled GCM. Contour interval is 0.05°C; warm (cool) shading indicates a warming (cooling), and the heavy line is the zero contour.

appears to be even more nonlinear than the intermediate model, with westerlies giving much stronger feedbacks than easterlies. Again, this is partly due to the changes in high-frequency mixing associated with the change in the climatology and the change in variability (discussed in Chapter 7). Finally, the GCM shows a more complex change in SST, with more off-equatorial structure than in the intermediate model.

5.7.2 Change in radiative forcing

We next test the "dynamical thermostat" hypothesis of Clement et al. (1996) and Cane et al. (1997). Recall that the intermediate model, which represented horizontal mixing as a constant diffusion and surface heat fluxes as a linear damping of SST anomalies, produces a *cooling* response to imposed uniform radiative heating, in accord with the dynamical thermostat. Will the hybrid GCM do the same?

To find out, we impose a weak uniform heating of 1 Watt m^{-2} over the entire basin in the GCM. The imposed heat flux is held constant and the model is integrated for 28 years. As before, the first four years of the run are discarded; only the last 24 years are analyzed.

The change in annual-mean SST for this case is shown in Fig. 5.17. There is warming nearly everywhere, but it is strongest away from the equator. The weakest warming occurs between 2–12°S and in the east Pacific between 2–7°N. There is a slight increase in the zonal SST gradient near the equator, but it is fairly small compared to the overall warming. The dynamical thermostat appears to be weak in this model, as it is in most GCMs.

To see why, we examine the equatorial structure of the response (Fig. 5.18). As in Fig. 5.16, all data have been scaled by the peak equatorial SST change, indicated above panel (b). Note that the coupled response to the imposed heat flux is weaker than in the intermediate model, even after accounting for the factor-of-ten difference in the strength of the forcing. The imposed heating induces a general warming, which gives a *westerly* response in the central basin despite the slight strengthening of the zonal SST gradient. These westerlies push the thermocline down in the east, which reduces $\partial_z T$ and leads to

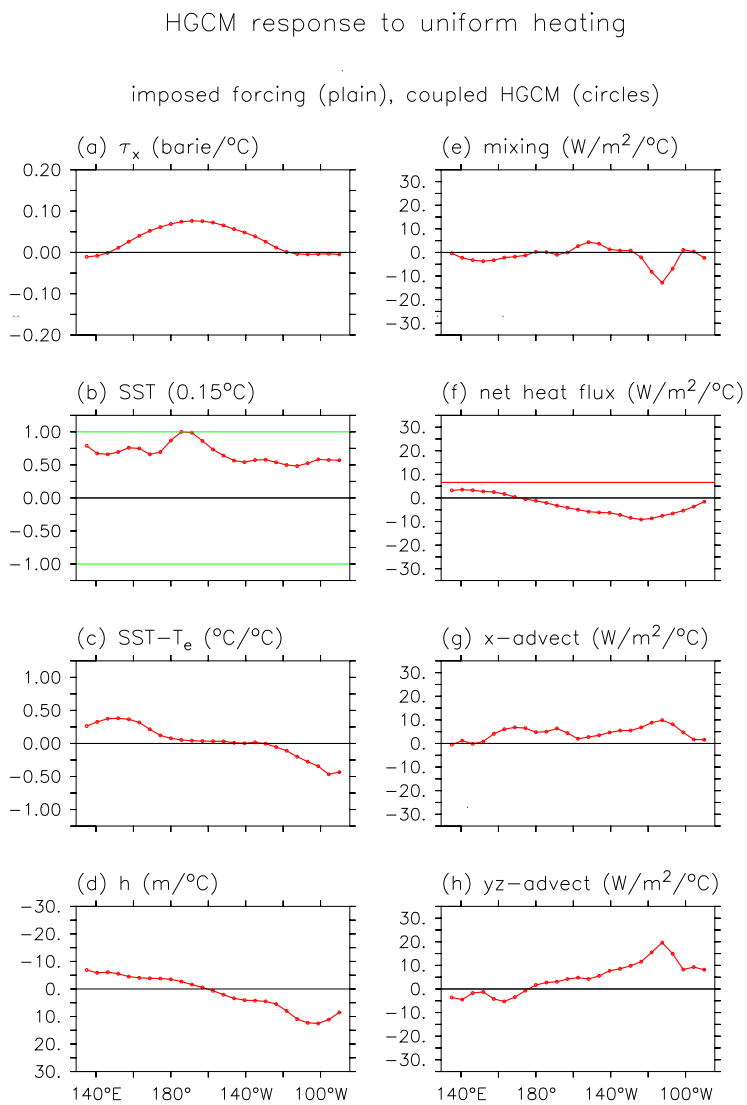

Figure 5.18: Response of the equatorial (2°S–2°N) climatology to an imposed uniform 1 Watt m^{-2} heating perturbation (plain line in panel f), as simulated by a hybrid coupled GCM. Fields are scaled by the peak SST change indicated in panel (b). Panels show the scaled change in (a) zonal stress, (b) SST, (c) temperature difference across the top 50 m, (d) depth of the 20°C isotherm (ordinate reversed); and the mixed layer heating due to (e) eddy fluxes, (f) surface fluxes, (g) zonal advection, and (h) meridional plus vertical advection.

Ekman-induced warming in the east. This eastern warming is countered by the increased cooling by heat fluxes and a reduction in heating from eddy fluxes. The SST warming also leads to an increase in $\partial_z T$ in the western Pacific, where increased cooling by Ekman and eddy fluxes helps to limit the surface warming. In the central equatorial Pacific, the feedback westerlies reduce upwelling and weaken the westward currents, which enhances the warming in that region. The warming of the ocean is more strongly damped by the surface heat flux feedback in the east than in the west.

It is clear from Fig. 5.18 that the changes in surface heat flux (and to a lesser extent, the eddy flux) are the primary reason for the increased SST gradient. Note that this is a rather different asymmetry-generating mechanism than in the intermediate model, where the surface flux acted to *damp* the enhanced gradient; in that case the gradient was generated by the entrainment cooling in the east, associated with the strong thermocline slope generated by *easterly* feedback stress. In the present case there is a *competition* between the zonal stress feedback (which acts to reduce $\partial_x T$) and the surface heat flux feedback (which acts to enhance $\partial_x T$). This competition produces little net change in the zonal gradient, and therefore limits the amplification of the perturbation by coupled feedbacks.

5.8 Discussion

The importance of feedbacks

This chapter has examined the sensitivity of the tropical Pacific climatology to perturbations imposed from outside the coupled system. A recurring theme is that these perturbations can be strongly amplified by coupled feedbacks. With the exception of imposed meridional stress, which produces hardly any coupled feedbacks in the intermediate model, most perturbations are accompanied by strong feedback zonal stress in the central Pacific and associated large changes in the east Pacific cold tongue.

Climate drift

This amplification by feedbacks means that even a good climate model with small dynamical errors can exhibit large climate drift. Consider an ocean model which is tuned to give realistic tropical SSTs when forced by one of the climatological wind stress analyses of Fig. 2.1. If the analyzed trades are weaker than they should be, then the tuned ocean model will be hypersensitive to the trade winds. Coupling such an ocean to a realistic atmosphere model would then give an equatorial cold bias which would be amplified by coupled feedbacks. The trade winds simulated by the CGCM would be too strong, not only compared to the (unknown) truth, but also compared to the analyzed stresses which were too weak in the first place.

Tuning

That the coupled feedbacks have a different pattern from the forced response raises an important point: the root of model bias may not be in the same place as the bias itself.

To improve the performance of a coupled model, one must think carefully about how model deficiencies may be seeding coupled feedbacks, and how those feedback effects are amplifying and redistributing errors throughout the simulation. Instead of tuning locally for the processes one most cares about (like regional SST or precipitation); it may be more effective to improve processes and fields (like central Pacific equatorial zonal stress) that most effectively seed coupled feedbacks, and processes (like equatorial upwelling) that set the strength and spatial structures of these feedbacks.

Attribution

A related issue involves attribution of climate changes that are observed in the real world and in paleoclimate data. The amplification and modification of small perturbations by coupled feedbacks may make it difficult to determine what change occurred and where it occurred. We have seen that a change in zonal stress off-equator, on the equator, or at different longitudes along the equator, and even a change in surface heat flux, can provoke similar responses from the tropical Pacific climatology. Thus it may not be possible to unambiguously deduce the causes of real equatorial climate changes without very detailed climate data and realistic model simulations.

Identification of model problems

In the intermediate model, the spatial structure of the coupled feedbacks appears to be determined mostly by the model dynamics, and not so much by the imposed perturbation. This is actually quite fortunate, because it implies that the feedback effects may be readily identifiable and easy to extract from a given simulation. Taking these results to their logical extreme, one may propose a "straw man" procedure for diagnosing problems in a coupled model.

Suppose one had a coupled climate model which was perfect in every way, except that it had an unknown problem which affected its wind stress field. Suppose that the error directly affected *only* the stress field, such that the direct stress error $\mathbf{E}$ could equivalently be viewed as arising from an external source; an example might be an incorrect value for the surface drag coefficient. Coupled feedbacks would tend to modify the stress error (and other dynamical fields) to produce a total stress bias $\mathbf{B}$ relative to the real world. If the coupled feedback response pattern $\mathbf{P}$ were known to be independent of the stress error, then the stress bias would be $\mathbf{B} = \mathbf{E} + f\mathbf{P}$ with f a scalar representing the feedback strength. The problem of diagnosing $\mathbf{E}$ would then be reduced to estimating f. One could imagine guessing an f, estimating the direct error as $\widehat{\mathbf{E}} = \mathbf{B} - f_{guess}\mathbf{P}$, imposing the opposite of this error in the climate model, spinning up the new climatology, and then diagnosing the new stress bias; repeating this procedure to find the minimum bias would then produce an optimal estimate for $\mathbf{E}$. In the example with an incorrect surface drag coefficient, $\mathbf{E}$ might exhibit patterns very much like the climatological stress, which would point to the drag coefficient as the source of the problem.

Such a procedure is useful mostly for its conceptual value, as it allows one to make quick mental estimates of where model errors lie. A more general procedure for finding model errors would be to compute the "flux adjustments" necessary to correct the model

climatology, say by spinning up the coupled model with a restoring to observations (e.g., Manabe and Stouffer (1988)). The flux adjustment fields would then give some indication of the direct error sources, and subtracting these adjustments from the unadjusted fluxes would give a measure of the structure and amplitude of the feedback error.

The observational network

Yet another issue has to do with the observational network. Naturally one would like to have good observations available at the "pulse points" where the coupled climate system is most sensitive to changes. The hybrid intermediate model suggests that the zonal stress in the central equatorial Pacific is one such key field. We have seen that the feedbacks in the intermediate model resemble those responsible for ENSO and the warm pool/cold tongue climatology, which suggests that one may be able to deduce the active feedback structures simply by observing the natural climate variability of the coupled system. This is fortunate, since it implies that the extensive observing system currently in place to study ENSO may also be extremely useful for detecting longer-term climate changes. It also suggests that paleoclimate data in these regions may be unusually useful in detecting and deducing past climate changes. It is important to remember, however, that the intermediate model indicates that the off-equatorial wind stress can also influence the equatorial climatology. Although this influence is small, it is probably important enough to warrant its consideration in modeling and forecasting of the equatorial Pacific.

Model dependence

As shown in Section 5.7, the climate change resulting from a given perturbation, and the mechanisms that produce this change, can be rather model-dependent. The great strengths of the HGCM are its more realistic treatment of the ocean (including eddy fluxes), its more sophisticated treatment of the surface heat fluxes, and the inclusion of the seasonal cycle. However, some of these assets might conceivably be liabilities as well, e.g. if the mixing parameterization were incorrect (a possibility, given the OGCM's climatological cold bias), or if the single-mode linear atmosphere model were inappropriate for the climate sensitivity experiments (since the positions of the wind stress and surface heat flux responses are fixed in space). The main strengths of the intermediate model, on the other hand, are its more flexible treatment of the wind stress response to SST anomalies, and its well-tuned (albeit very simple) dynamics.

Simplicity of the climate manifold

That the coupling produces similar climate change patterns in the intermediate model for different imposed perturbations greatly simplifies the study of ENSO sensitivity to climate, since the problem is largely reduced to mapping the ENSO response to "El Niño-like" and "La Niña-like" climate states. For a given climate perturbation, one can simply refer to the climatology scale (above panels (b) in the equatorial structure diagrams) to deduce the structure and amplitude of the change in the mean state, and then use this index assess the ENSO response from the sensitivity diagrams that will be presented in

Chapter 7. It is hoped that together, these diagrams will prove quite useful to both theorists and climate modelers.